Geoelectrical Characterization of Sulphate Rocks

Ander Guinea Maysounave

Programa de Doctorat de Ciències de la Terra

GEOELECTRICAL CHARACTERIZATION OF SULPHATE ROCKS

Ander Guinea Maysounave

2011

Advisors / Directors de tesi:

Drs. Elisabet Playà Pous & Lluís Rivero Marginedas

Departament de Geoquímica, Petrologia i Prospecció Geològica

UNIVERSITAT DE BARCELONA

Methods and Limitations

Ander Guinea 2011

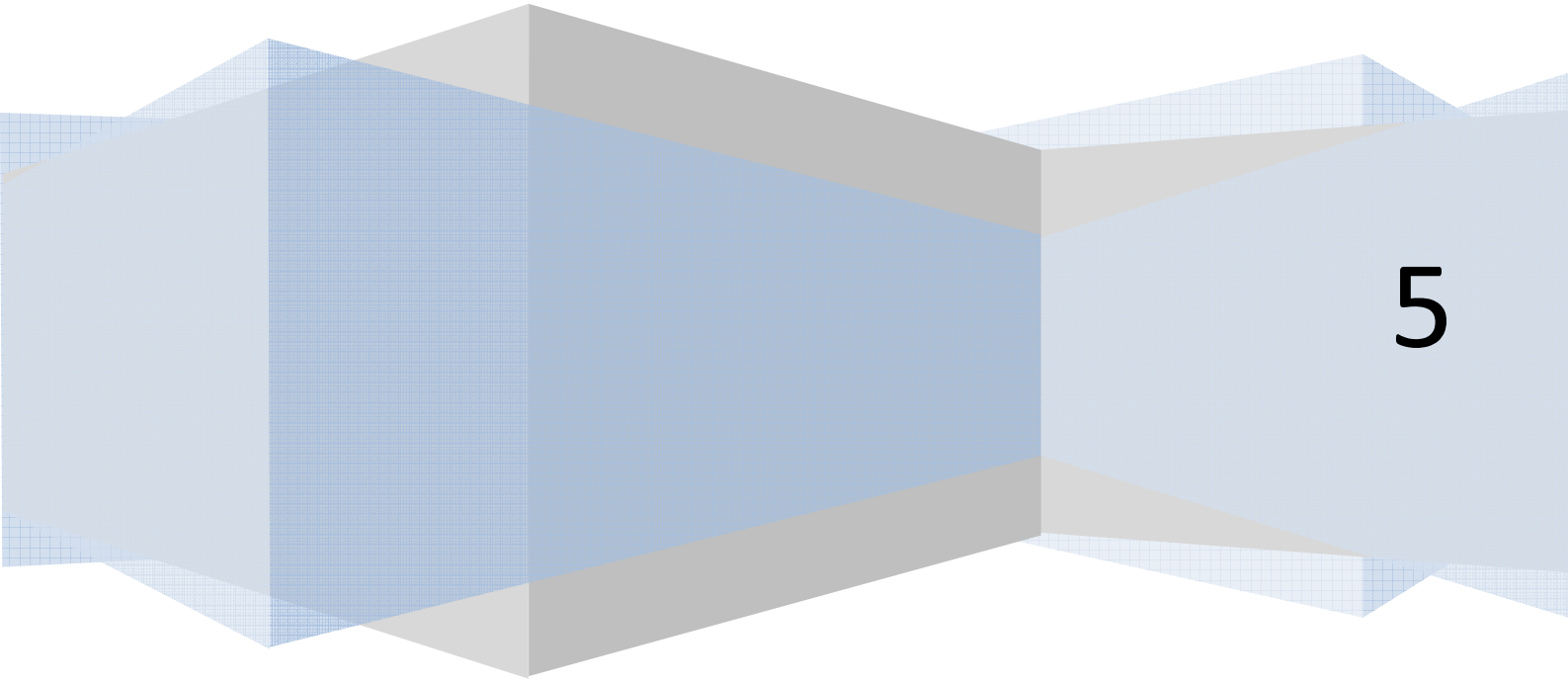

5

.1 STRUCTURES IN SULPHATE ROCKS

.1.1 Introduction

In this section, the most common structures which can be found in sulphate rocks are analyzed. Due to the solubility of sulphate minerals, secondary porosity can be developed. This porosity has different degrees; from centrimetric tunnels to a regional karstification. In the field, it is possible to find these structures as old karst filled with lutitic sediments (figure 5.1A), or as hollow cavities (figure 5.1B). From the geoelectrical point of view, the response of the terrain will be very different having one case or another. In the case of filled karst, the infilling materials are lutites and some gypsum blocks; this will decrease the resistivity in the area, making the gypsum layer discontinuous. In the case of having a tunnel, the resistivity of the air is very high (tends to infinite), so it can be identified due to its high resistivity value.

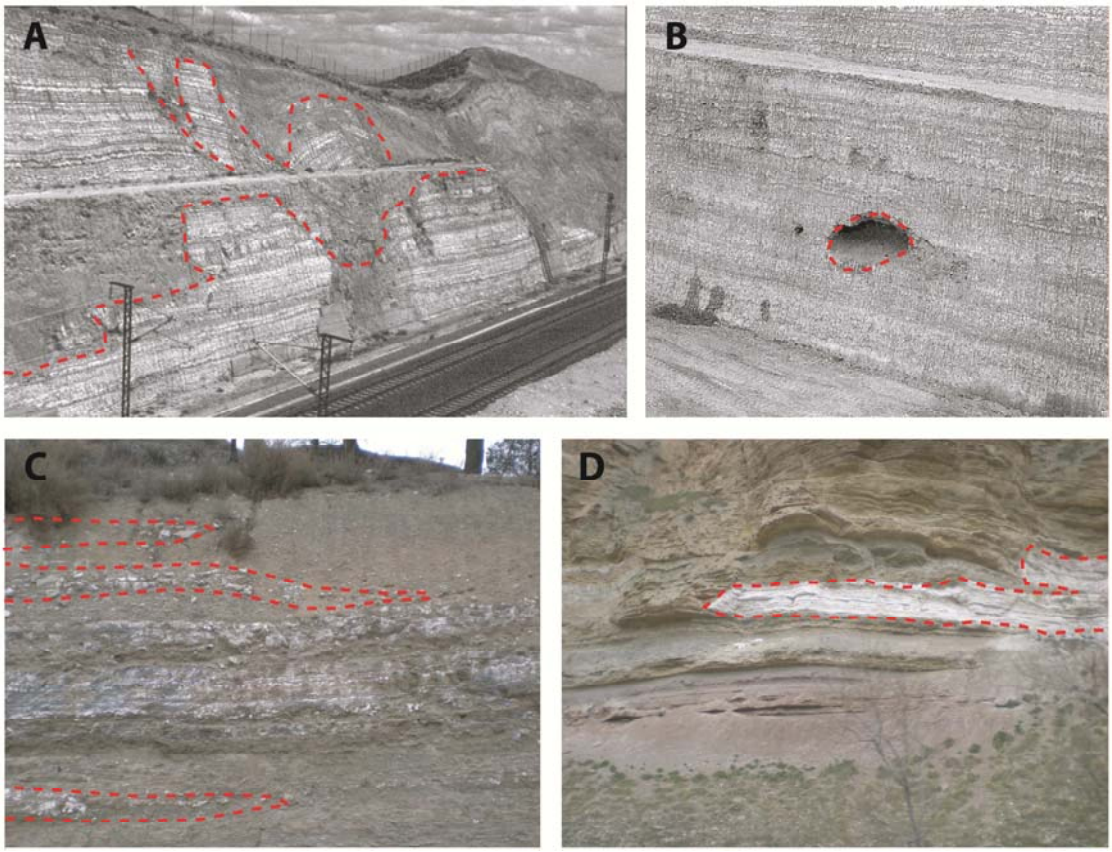

Figure 5.1: Photographs of the most common structures in sulphates. A) Gypsum karstification filled with lutites (modified from Guerrero et al. 2004); B) Dissolved tunnel in a gypsum formation (modified from Guerrero et al. 2004); C) Lateral variations in gypsum layers; D) Glauberite pure layer disappearing laterally.

Besides the secondary-porosity structures; sulphate rocks, as other evaporitic materials, usually display lateral variations of purity originated during their deposition (primary structures). These changes can be gradual (figure 5.1C) or sharp (figure 5.1D). These structures generate lateral resistivity variation of the sulphate layers (depending of their purity). Additionally, old sulphate sequences can be folded or faulted generating complex structures as diapires and making the resistivity interpretation more difficult.

.1.2 Theoretical models: methods

In order to check the way in which the structured mentioned before affect to the resistivity distribution of the terrain; 4 model blocks have been elaborated with RES2DMOD program (figure 5.2). These models simulate typical structures with different complexity and from them direct models have been calculated. The data has been processed afterwards with

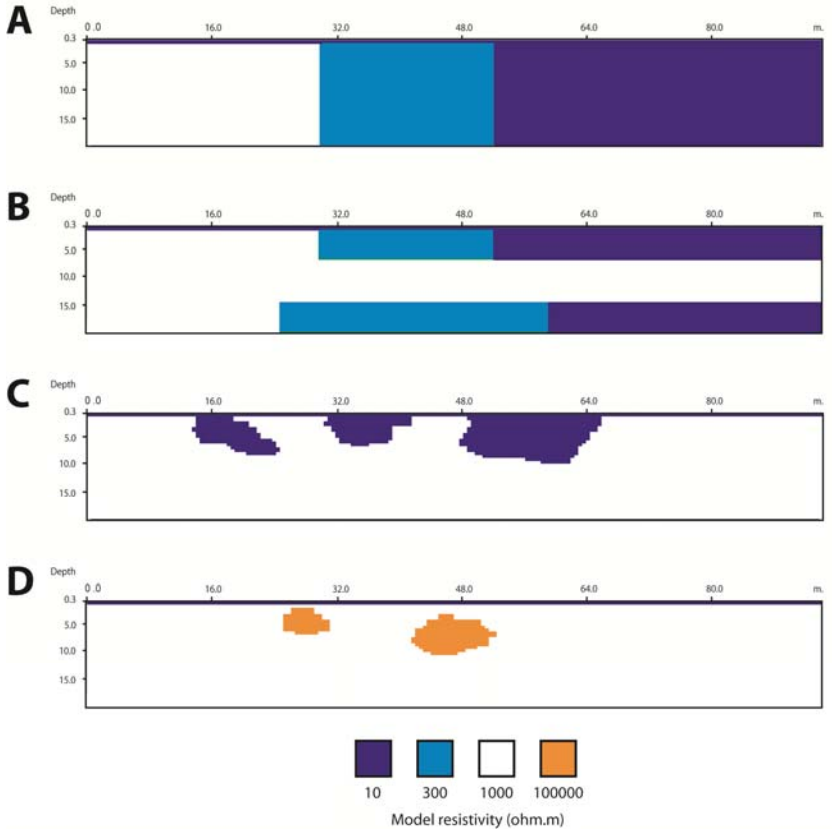

Figure 5.2: Model-blocks representing typical structures in sulphate rocks. White color represent pure gypsum, light blue impure gypsum and dark blue lutites. The cavities are represented by orange color. A) Simple lateral variation; B) Complex lateral variation; C) Filled karst; D) Cavities in gypsum.

the program RES2DINV. The used array has been either Wenner-Schlumberger or Dipole-Dipole, depending of the suitability of each case. The selection of the array in the geoelectrical surveys performed in sulphate rocks is further discussed in the next section of this chapter. The electrode spacing is 2 meters with 48 electrodes. The obtained results have been compared with structures obtained in different ERT profiles performed during the elaboration of other chapters.

The first model (figure 5.2A) represents a simple lateral purity change, while the second model (figure 5.2B) display a complex purity change in various levels, as it is shown in figure 5.1C. The last two models are dissolution structures with a karst infilling (figure 5.2C) and cavities (figure 5.2D). All these structures have been considered to be developed upon pure gypsum (1000 ohm.m); but they could be developed upon other sulphate rocks and with different purities. The resistivity value selected for the cavities is the maximum which can be selected by the program RES2DMOD: 10^5 ohm.m (this value is higher than any geologic material).

.1.3 Results and discussion

The inverted resistivity profile of the first model (figure 5.3A) displays a gradational resistivity change from left to right; this is, from pure gypsum rocks to lutitic ones. The sharpness of the resistivity change depends on the presence of intermediate purity rocks. This type of structures are shown in some of the profiles performed in gypsum formations in chapter 3 (section .1.2), but the best example is shown in the survey of Pira gypsum unit of the next chapter (section .1). The resistivity section of the more complex lateral changes-model shows vertical resistivity variations (figure 5.3B). The uppermost lateral change is well defined, while the bottom layer is not shown. This is because in the bottom part of the profile the sensitivity of the ERT is low. In any case, this disposition of the sulphate layers may generate complex resistivity changes. Complex lateral changes similar to the ones displayed in this model have been shown in the glauberite deposit of Zaragoza in section .3.2 of chapter 4. The complexity of the lateral changes, in many cases depends on the scale of the survey; simple changes in short profiles may be complex in long profiles.

The inverted profile of the model displaying a karst structure filled with lutites, shows the dissolved surface by means of low resistivity (10 ohm.m) areas (figure 5.3C). This structure generates some circled shapes in the uppermost gypsum materials; which could lead to a

misleading. Karstic infilling examples have been shown in the glauberite study of Zaragoza, in the profiles of B4, B10 and C1 boreholes (figures 4.32B, C and D in chapter 4.3.3.3). The last model shows two cavities in a gypsum layer; this is well defined in the resistivity image (figure 5.3D). Due to a sensitivity matters, the cavities only will be detected in shallow positions (because they are resistive bodies within other resistive body). An example of a cavity in sulphates is displayed in the profile E (figure 4.18E) of chapter 4.

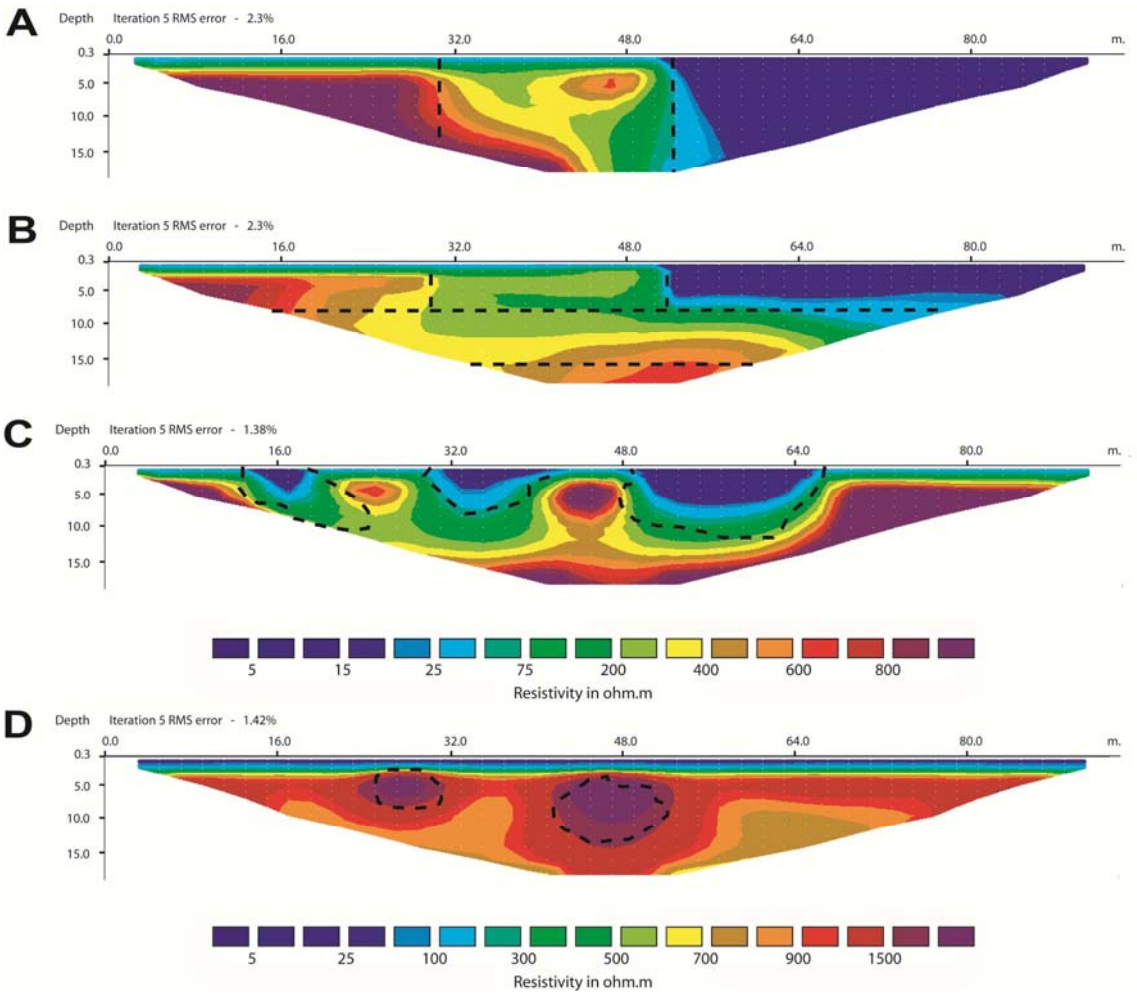

Figure 5.3: Inverted resistivity profiles of the direct models obtained from figure 5.2. The resistivity changes in the original models are marked with dashed lines.

.2 SELECTING THE ARRAY

.2.1 Introduction

One of the most relevant points in ERT surveys is to choose a suitable electrode- array configuration. The best definition of the structure which is under the target depends on it. There are many different 2D and 3D arrays (about 100) which have ever been used in the electrical prospecting methods. We have chosen the Dipole-Dipole and Wenner-Schlumberger arrays, due to their adequate investigation depth (approximately the fifth of its horizontal extension) and sensitivity to resistivity variations (Orellana 1972). Depending on the sensitivity of the array, lateral and vertical resistivity variations will be differently displayed. In some cases in which these variations exists, they will not be shown in the inverted images due to the limitations of the method.

Once the data has been acquired and processed, the proper interpretation of the electrical imaging is essential. On this purpose, criteria for checking the reliability of the model have to be found in order to detect possible artifacts.

.2.2 Methods and Theory

Structurally well known areas have been studied with ERT using Dipole-Dipole and Wenner-Schlumberger arrays in Vilobí del Penedès and Cantallops (NE of Spain). The previous knowledge of the structures and the blocks relative-sensitivity imaging has been used as reliability criterions. RES2DINV program has been used to carry out the inversion process. The program divides the pseudosection into blocks and calculates the Jacobian matrix (J) using a finite element subroutine (Locke and Baker 1996; equation 5.1):

Equation 5.1: $J=\partial p/\partial n$

Where p is the value of the calculated matrix and n represents the different parameters. This matrix represents the sensitivity of the different blocks. The relative blocks sensitivity distribution is directly related to the changes in the model for each iteration and therefore, with the final real resistivity image. Direct models have been also performed with the RES2DMOD program simulating the same structures in order to compare with the results obtained in field for both resistivity and relative-sensitivity distribution.

.2.3 Sensitivity analysis

The sensitivity of both Dipole-Dipole and Wenner-Schlumberger arrays has been theoretically calculated for homogeneous and layered terrain (with a change of resistivity at depth of 5 meters). For a homogeneous terrain, the sensitivity of the model blocks in the Dipole-Dipole array is lower in the deepest part in comparison to the Wenner-Schlumberger array (figure 5.4). In the case of the layered terrain, the main difference between these two arrays is shown where the most conductive layer is below the resistive one (figure 5.5). In the case of the Dipole-Dipole array, the relative sensitivity within the blocks of the conductive body experiments an important increase, displaying a relative maximum value. The Wenner-Schlumberger array shows a slight change, being more similar to the case of the homogeneous terrain. This has been calculated elaborating a 2-layer terrain model with RES2DMOD program, which calculates the electrical apparent resistivity pseudosection for a user-defined 2D subsoil model (Loke 2002).

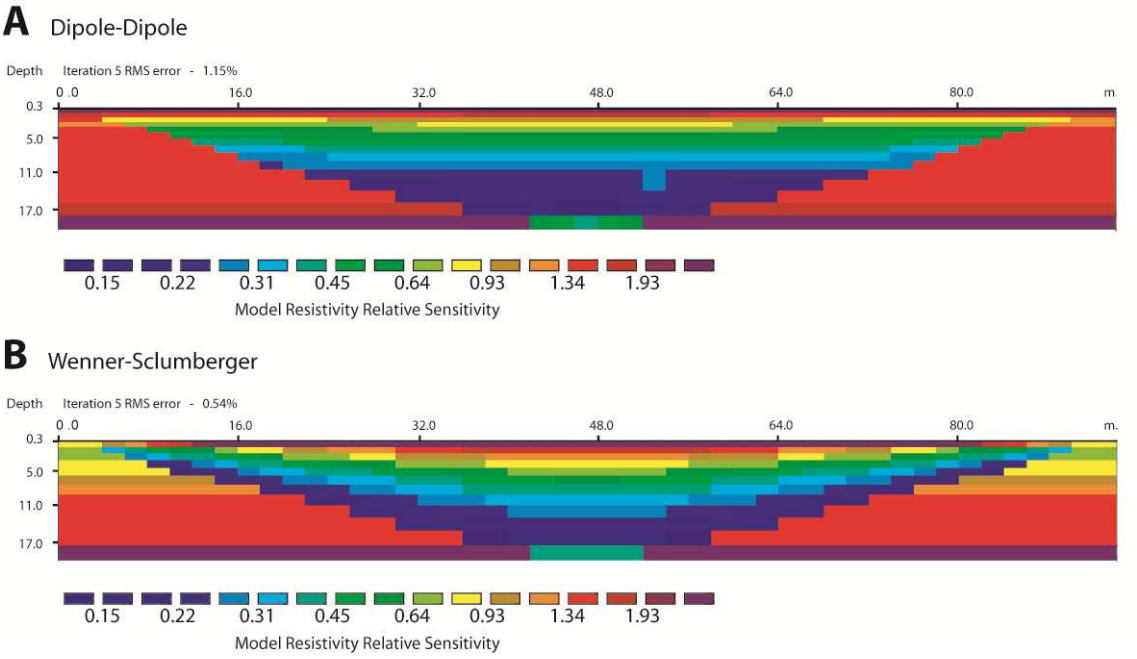

Figure 5.4: Relative-sensitivity block distribution for the cases of A) Dipole-Dipole and B) Wenner-Schlumberger arrays.

The blocks relative-sensitivity distribution is directly related to the changes in the model for each iteration and therefore, to the final real resistivity image. As different models

can be calculated for the same apparent resistivity pseudosection, the reliability of the product of the inversion process has to be checked.

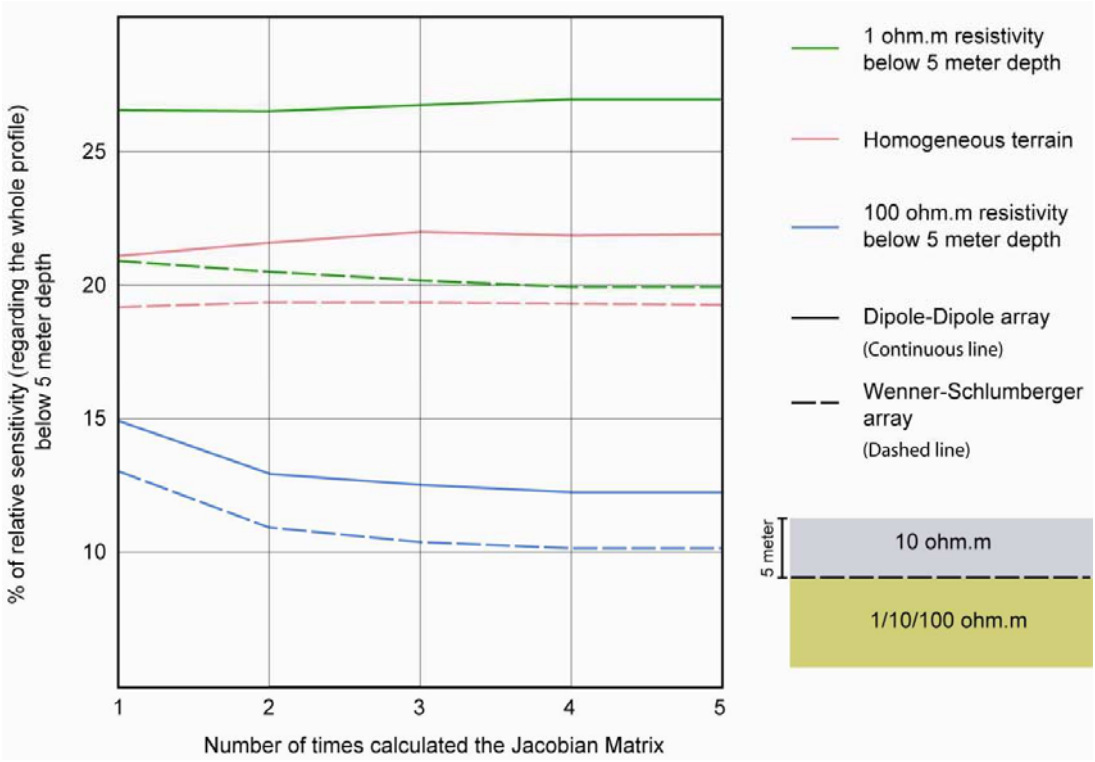

Figure 5.5: Variations of the % of blocks relative-sensitivity due to vertical differences of resistivity for both Dipole-Dipole (continuous line) and Wenner Schlumberger arrays (dashed line) with a separation of 2 meter between electrodes. Two layer terrain-model has been elaborated with RES2DMOD program (bottom right of the figure) and then the data has been inverted with RES2DINV, using different number of calculations for the Jacobian matrix. In the iterations without Jacobian matrix calculation, the program uses a quasi-Newton approximation.

.2.4 Field and theoretical examples

The Vilobí Gypsum unit is located close to the Vilobí del Penedès village (Barcelona, Spain; figure 5.6A); this unit is overlaid by lutites and limestones. The ERT profiles revel that the gypsum level display high resistivity values at depth, close to 1000 ohm.m. Outcropping limestones have lower values (between 100 and 200 ohm.m). The intermediate arch-shaped lutite layer is a conductive level with electrical resistivity values below 10 ohm.m. The lutite layer is at the bottom of the investigation depth. In these cases it is recommended to use arrays such Wenner or Wenner-Schlumberger because they are more sensitive to vertical variations on the resistivity value of the terrain. On the other hand, Dipole-Dipole array has

higher sensitivity to lateral variations and lower block-sensitivity values at depth; therefore it is not supposed to be reliable in the lower half of the electrical resistivity image.

Both arrays were tried in this structure. The inversion routine was performed calculating the Jacobian Matrix thrice (for the first 3 iterations). The result shows that Dipole-Dipole array define better the structure comparing to Wenner-Schlumberger profile (figures 5.7A and B). The image of block relative sensitivity displays a relative maximum in the value within the lutite layer, especially marked in the case of Dipole-Dipole array. This is coherent with the influence of conductive materials shown in the figure 5.5, where low resistivity materials at depth generate large block relative sensitivity increasing. In any case, both arrays display coherent resistivity distribution and no artifacts are generated.

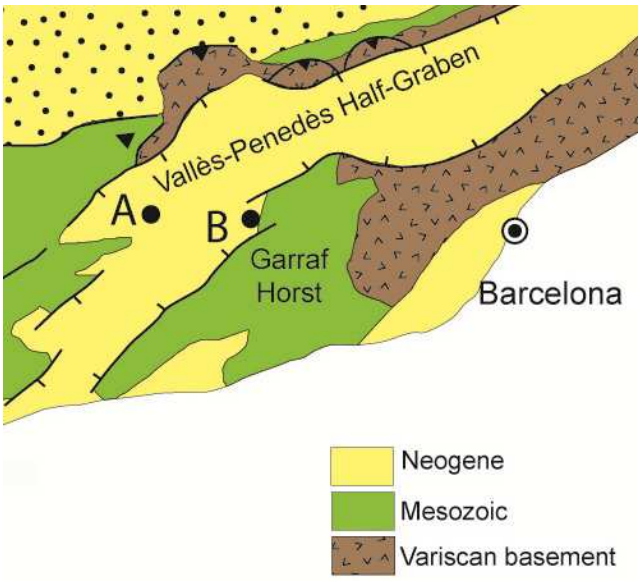

Figure 5.6: Situation of the profiles in the Vilobí Gypsum unit (A) and graben structure in Cantallops (B) in the Vallès-Penedès basin (modified from Travé et al., 2009).

A direct model calculation has been performed with a theoretical homogeneous terrain of 10 ohm.m resistivity value crossed by similar arched layer (1 ohm.m resistivity value). After the inversion, the images show the same trend as in the case of Vilobí section for both resistivity and block relative sensitivity sections (figures 5.7C and D).

Other profile has been tried in another location with different structure. Close to the village of Cantallops (Tarragona, Spain; figure 5.6B) graben-like structures were developed

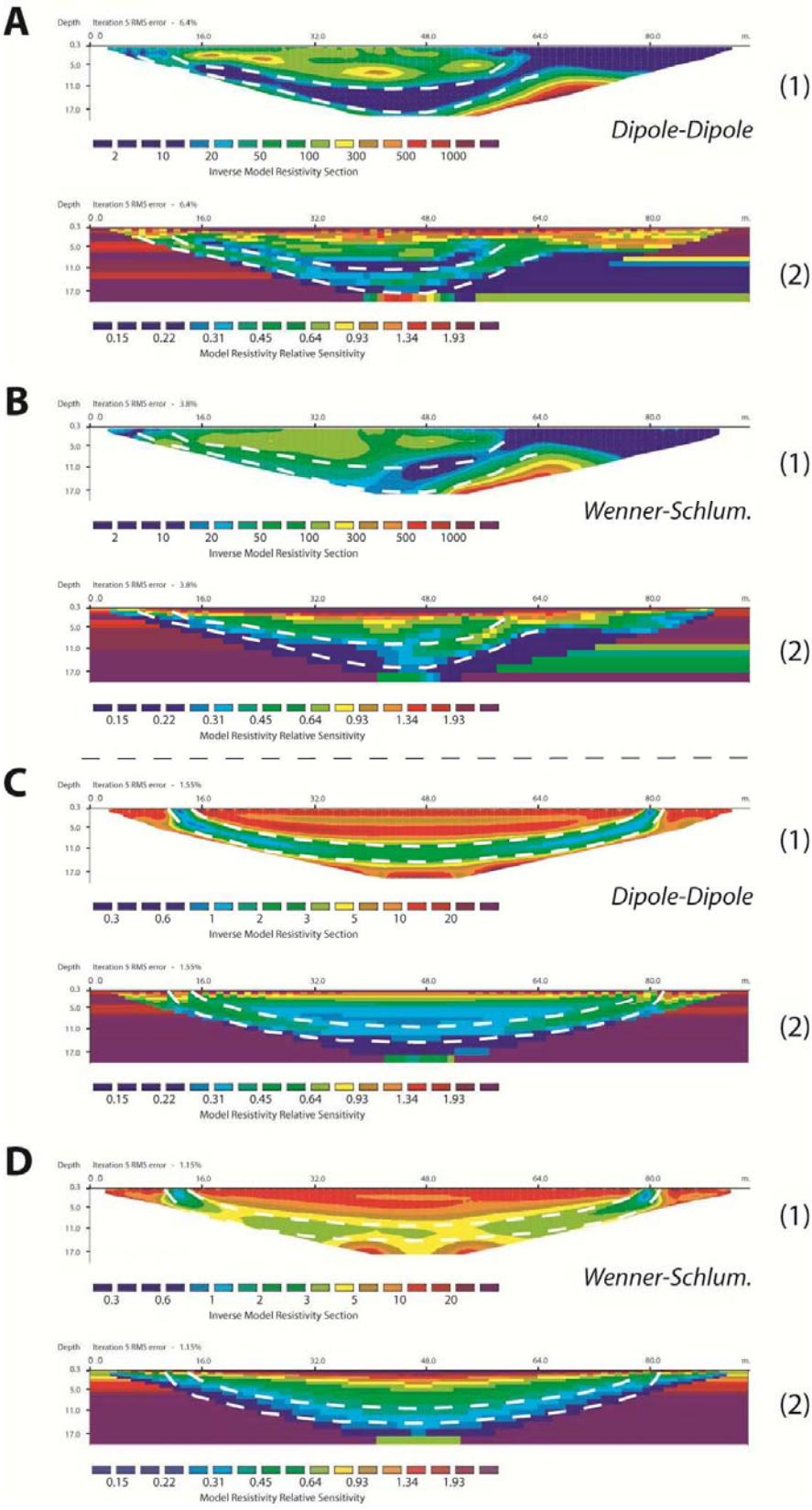

Figure 5.7: Resistivity (1) and block relative sensitivity (2) sections of Vilobí del Penedès field example (A and B) and arched-layered model (C and D) for both Dipole-Dipole and Wenner-Schlumberger arrays. The known conductive layer is represented by dashed white lines. The image of resistivity of Dipole-Dipole array fits better to the conductive layer and the sensitivity one displays a relative sensitivity increasing within it.

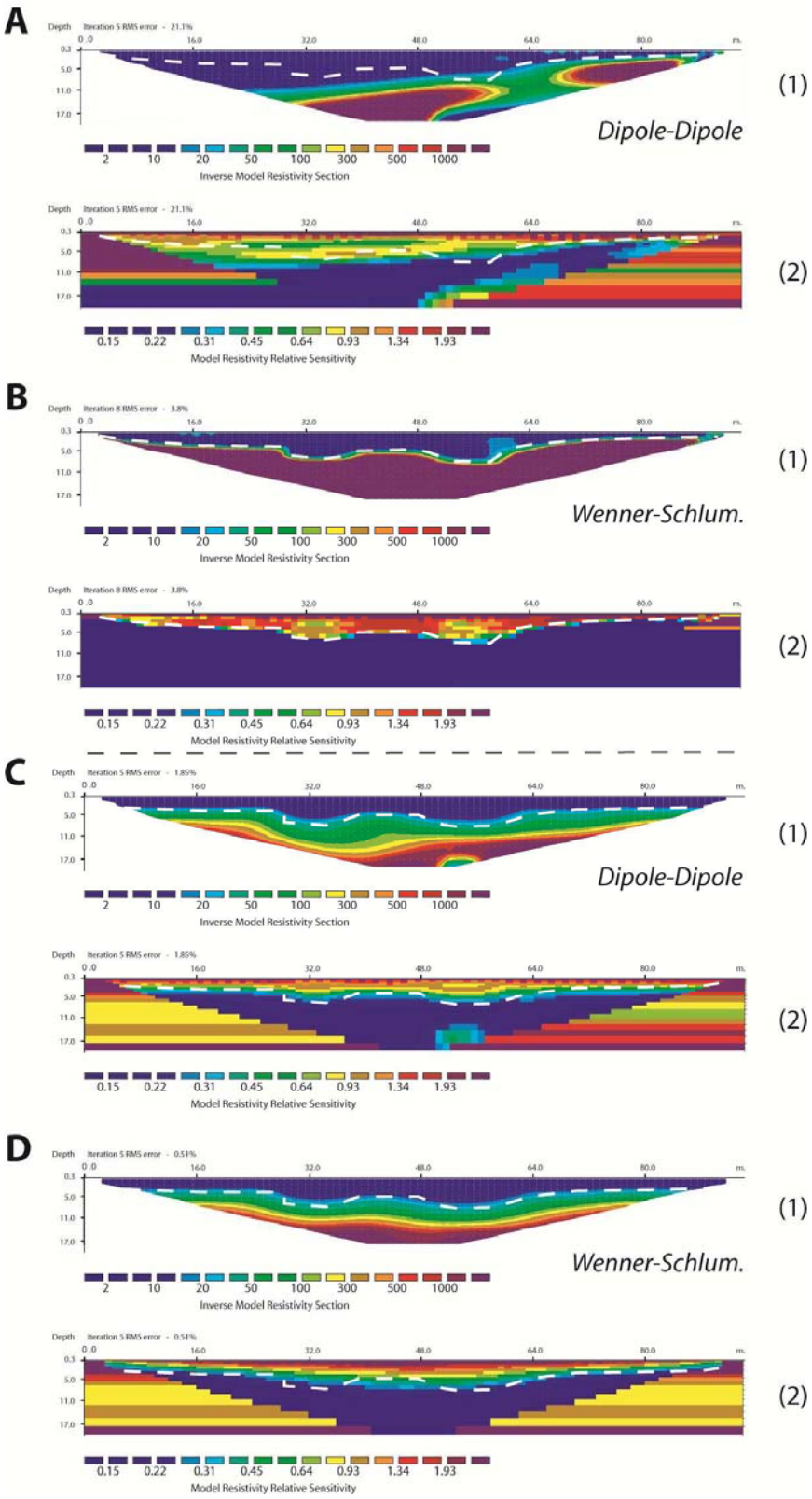

Figure 5.8: Resistivity (1) and block relative sensitivity (2) sections of Cantallops field example (A and B) and stepwise model (C and D) for both Dipole-Dipole and Wenner-Schlumberger arrays. The boundary between layers is represented by dashed white lines. The images of resistivity of Dipole-Dipole array display artifacts in their bottom-right zone while these artifacts are not shown in the Wenner-Schlumberger cases.

during the Miocene extension. In one of these grabens, an ERT survey has been carried out. The structure is formed by faulted limestones overlayed by lutites. In this case the conductive materials are above. The Wenner-Schlumberger profiles shown better results in comparison to the Dipole-Dipole images, which show low resistivity values at depth with low sensitivity values. A stepwise model similar to the Cantallops structure has been elaborated and the direct model has been calculated. Dipole-Dipole array has shown artifacts in a bottom corner of the resistivity image where the sensitivity value is low. Dipole-Dipole array tends to generate artifacts in the bottom part of large homogeneous bodies due to its asymmetrical relative sensitivity distribution as is shown in the case of homogeneous terrain (figure 5.4A).

When there is a great contrast of resistivity in the terrain and the most resistive layer is at the bottom, the sensitivity of the method focuses in the more conductive upper layer. When processing this data, to perform a big number of iterations improves the definition of the shape of the boundary between the two layers as it is shown in the case of Cantallops profile (figure 5.8B). In this case 9 iterations where performed and the different steps of the graben structure are well shown. The problem of performing a great number of iterations when there is a zone with very low relative sensitivity (this is, a large value of resistivity zone in contrast with conductive ones) is that the calculation of the real resistivity value increases giving anomalous values. In the case of Cantallops profile (figure 5.8B) the representation only displays that the limestone layer has more than 1500 ohm.m, but the calculated values are close to $2x10^5$ ohm.m, arriving to more than $4x10^7$ ohm.m in some areas. These large values are achieved due to that variations in these low sensitive zones do not affect the stability of the calculation of the whole section. If the contrast of the resistivity is smaller, the sensitivity distribution is more similar to the one shown in figure 5.4. Graben structures are not present in sulphate rocks, but this is a good example of processing complex resistivity boundaries.

Because of sentivity matters, is possible to calculate resistivity values of anhydrite or larger ones for gypsum units when they are in the bottom of the profile below a conductive layer. An example of this is shown in the next chapter for the case of Pira gypsum survey. To minimize the effect of the increasing of the resistivity value calculation in low sensitive zones; is better to perform a minor number of iterations of the model if it converges. The program usually converges between iterations 4 and 6 and normally there is no significant reduction of the RMS error after iteration 5 (nor significant changes in the final section). Because of this, most profiles in this thesis have been processed with 5 or 6 iterations. If this convergence is not achieved, the iteration process should continue.

As mentioned before, there are many other electrode arrays which are commonly used in ERT acquisition (Pole-Pole, Pole-Dipole, Gradient, among others…), but in general these arrays will show a similar trend of sensitivity to either Dipole-Dipole or Wenner-Schlumberger. This will depend on if they are more sensitive to lateral or vertical variations on the resistivity distribution.

.2.5 Limitations

In chapter 4 the differences of electrical conductivities between different sulphate rocks have been discussed. It has been established that pure gypsum rocks have a resistivity of 10^3 ohm.m and 10^4 ohm.m for anhydrite, while glauberite has an intermediate value. If we consider the effect of the matrix, the values of resistivity between different rocks may overlap; making them impossible to distinguish without additional information (as parametric boreholes). Besides, because of the limitations of the used geoelectrical method, it is possible to not achieve the identification of different sulphate rocks.

In the previous section, the sensitivity of ERT profiles has been analyzed. When there is a large resistivity contrast between the layers of the terrain, the relative sensitivity of a ERT profile concentrates in the less resistive formation (as it has been showed in figure 5.5). A typical case of a sulphate deposit is a pure multiphase sulphate formation (with any combination of gypsum, anhydrite and glauberite rocks) underneath a lutitic quaternary sedimentary basin. Under these conditions, the relative sensitivity of the method increases in the lutitic layer while it decreases in the sulphate rocks; making impossible to distinguish between them. The differentiation of sulphate phases will be only possible in the case of having a very thin lutite layer. In the study of anhydrite rocks under field condition in section 4.2.2, the sulphate rocks were in general very close to the surface and because of this, it has been possible to identify them.

As an example of these limitations, 4 simple numerical models have been elaborated with RES2DMOD program. Models 1 and 3 (figure 5.9A) represent a horizontal lutitic basin with a thickness of 5 or 1 meter respectively; with a pure gypsum deposit below. Models 2 and 4 (figure 5.9B) have the same materials and geometry, but with an 18 meter wide anhydrite rectangle situated in the center part of the gypsum layer. Direct models have been elaborated for both Wenner-Schlumberger (WS) and Dipole-Dipole (DD) arrays. The used electrode spacing has been 2 meter, with a total of 48 electrodes and a maximum investigation depth of

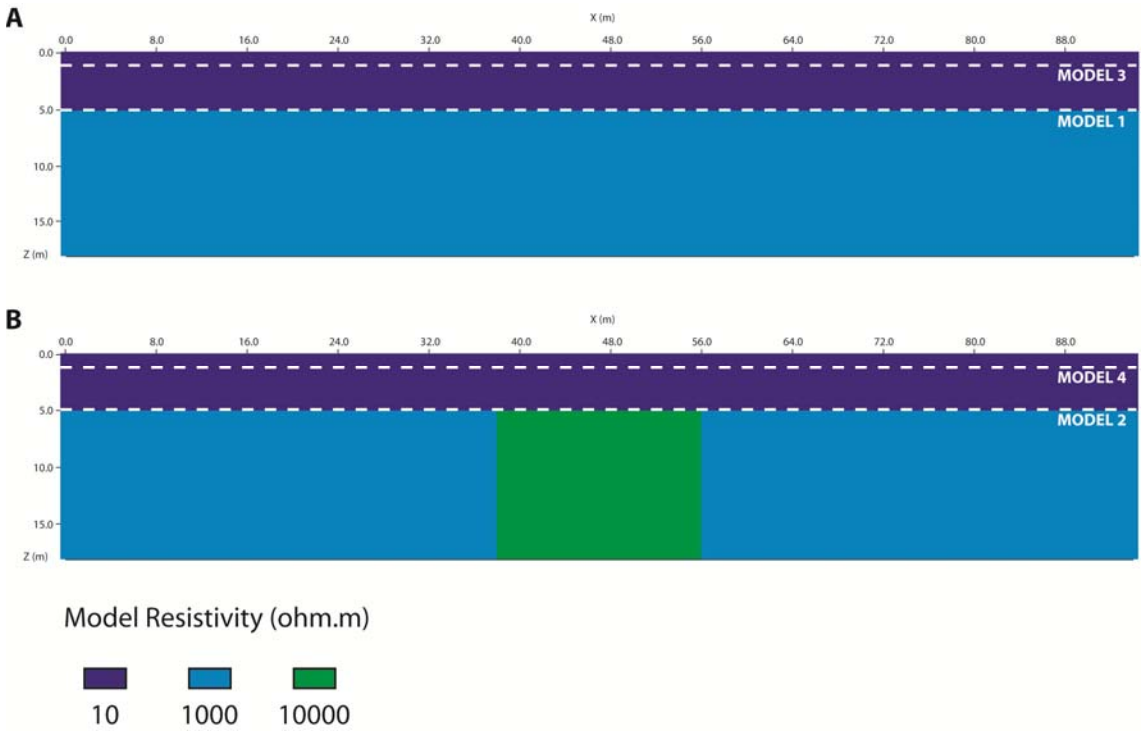

Figure 5.9: Theoretical terrains with sulphate rocks below a lutitic layer elaborated with the program RES2DMOD. A) Lutite layer (dark blue) with pure gypsum (light blue) below; B) Lutite layer with pure gypsum and anhydrite (green) rocks below. For models 1 and 2, the sulphate layer is at 5 meter depth, while it is at 1 meter depth (marked with dashed line) in the case of models 3 and 4.

approximately 18 meter (depending on the array selected).

The whole data set has been inverted with RES2DINV program and the results show different structures. In the case of model 1 (5 meter-thick lutite layer with a pure gypsum body underneath) both WS and DD arrays show the resistivity change with a progressive value increasing with depth (figure 5.10A and C); in the case of DD the values are lower in the bottom. In model 1, the relative sensitivity within the gypsum layer is 9 and 11% of the total for WS and DD respectively (table 5.1). Model 2 has the same structure but with an anhydrite body in the middle of the gypsum unit; the relative sensitivity in the sulphate layer is 8 and 9 for WS and DD arrays respectively (table 5.1). The relative sensitivity is very similar to the one observed for gypsum layer in model 1, this is, very low. Because of this, nor WS or DD arrays show lateral variations in the bottom-sulphate layer (figure 5.10B and D). The sections obtained are very likely to the ones of the model 1; in the case of DD array the resistivity in the bottom has increased with respect of the section of model 1, but not enough as to distinguish lateral resistivity variations in the sulphate body. Thus, gypsum and anhydrite phases appear as a single layer.

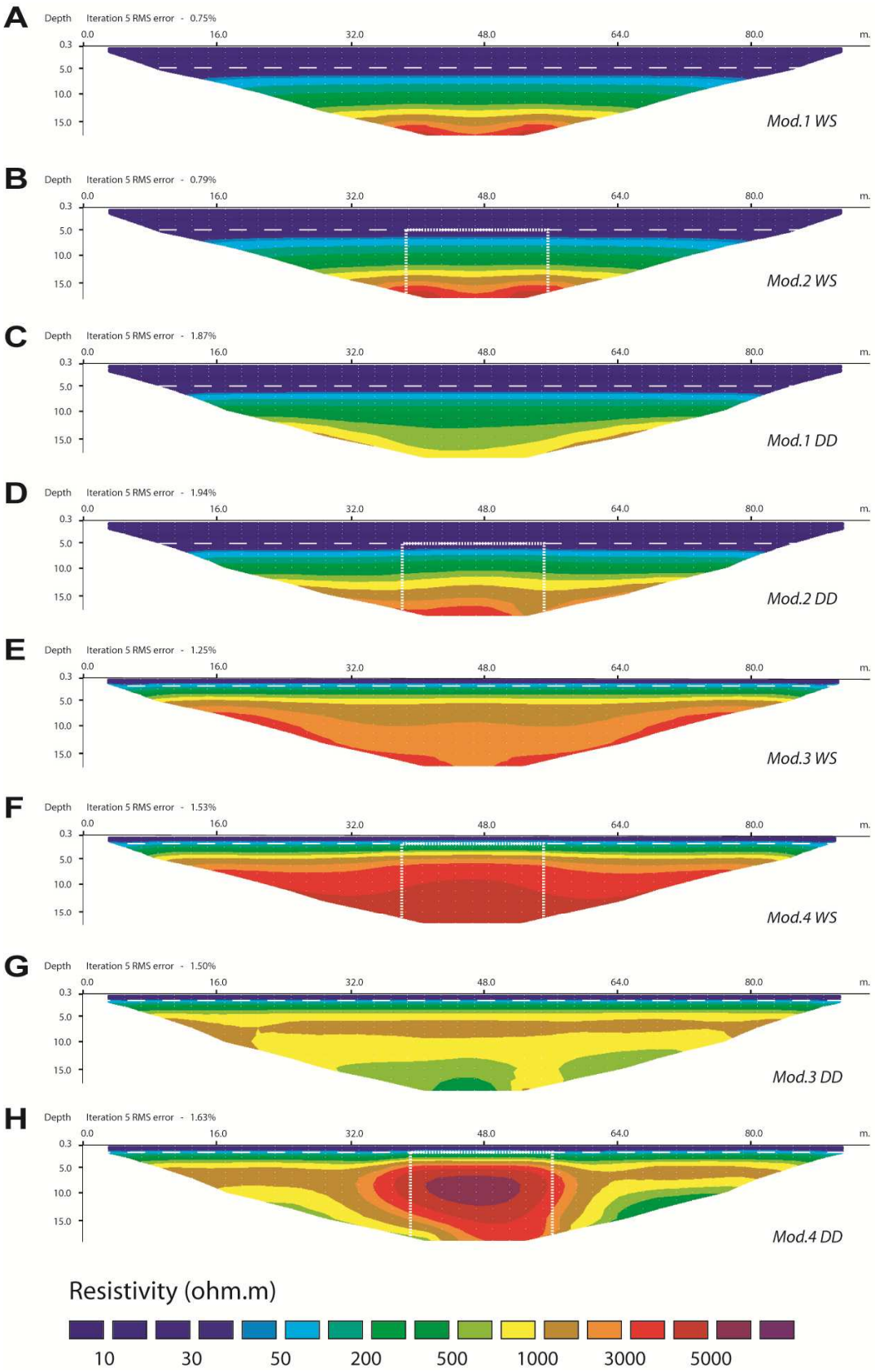

Figure 5.10: Inverted sections from the direct models (Mod.1-4) calculated with the models described in figure 5.9 for both Wenner-Schlumberger (WS) and Dipole-Dipole (DD) arrays. The dashed lines represent the boundary between the lutitic layer and the bottom sulphate rocks and the dotted lines represent the situation of the anhydrite body when present.

Model 3 is similar to model 1 but the width of the lutite layer is much thinner; only one meter thick. The relative sensitivity in the gypsum layer is larger than in the previous models for WS with 35%, and especially for DD with 43% (table 5.1). Both arrays define perfectly the transition between the lutite layer and the gypsum (figure 5.10E and G), but in the case of DD there are some artifacts in the bottom part. In the case of model 4, which is similar to model 3 but with an anhydrite body in the center part of the gypsum deposit, the lateral transition between sulphates is defined for DD array (figure 5.10H). The WS array shows a resistivity increasing trend in the center part (figure 5.10F), but the sulphate layer appears as quite homogeneous. In this case the more sensitive nature of DD to lateral changes makes the difference. The relative sensitivity in the sulphate layer for both arrays is similar to the one displayed in model 3, this is, 35 and 41% for WS and DD respectively (table 5.1).

Model	R. Sens. in lutite (%)	R. Sens. in sulphates (%)
1 WS	91	9
1 DD	89	11
2 WS	92	8
2 DD	91	9
3 WS	65	35
3 DD	57	43
4 WS	65	35
4 DD	59	41

Table 5.1: Relative sensitivity distribution in lutite and sulphate layers for the direct models calculated from figure 5.9 after 3 Jacobian matrix calculations.

With this example it has been showed the impossibility of differentiating sulphate phases in low sensitivity conditions; the sulphate layer should be close to the surface (the depth depends on the length of the profile) if there are low resistivity materials above. In the case of sulphate rocks with low purity in their composition, the electrical resistivity value is lower and therefore the relative sensitivity is larger; increasing the possibilities of observing differences within the most resistive body. In this case we have analyzed the most extreme situation in which the sulphate rocks are considered to be 100% pure.

.3 EFFECTS OF HETEROGENEITIES IN TRANSITIONAL VALUES

.3.1 Introduction

In the previous chapter, the percolation phenomena in sulphate rocks has been explained. It has been considered that for any sulphate rock in their electrical resistivity range (depending on their composition) there are two domains: A) Matrix (or lutite) domain; in which the resistivity of the bulk rock is conditioned by the matrix; and B) Sulphate domain; in which the sulphate phases are dominant. Between these two domains it has been observed a transitional domain. From a theoretical point of view, it has been considered that the sulphate rocks have a relatively homogenous distribution of their components. This premise is an approximation to the reality; but in some cases the presence of heterogeneities may be larger. In the theoretical calculations for anhydrite in section 4.2.4 it has been observed differences for transitional values at microscale. The photographs of thin sections used for these calculations (figure 4.26) display a clearly heterogeneous distribution of the different phases. In some cases, it is possible to have gypsum deposits with this type of heterogeneities at larger scale; affecting the electrical resistivity value of the rock.

.3.2 Transitional domain

In a theoretical rock formed with perfect microspheres of sulphate embedded in a perfectly homogeneous lutitic matrix, the transition between the sulphate and the matrix domains would be infinitesimal; no transitional value would exist. In the theoretical calculations performed to calculate the resistivity value of gypsum rocks (section 4.1.4), the gypsum blocks have been elaborated as little squares of pure gypsum with a equally squared lutitic matrix with 1000 and 10 ohm.m respectively (figure 4.10). The results have shown a trend of resistivity with a transitional value for rocks between 55 and 75% in gypsum purity. The field data and laboratory essays have shown a similar trend, so this transitional domain can be considered a good approximation for a general case.

As mentioned before, it is possible to have a more heterogeneous distribution of the components in the sulphate rocks. When these heterogeneities are large, they can be considered as a different rock (for example a gypsum-rich lutite body within a larger pure gypsum host-rock), but in the case of metric scale, heterogeneities below the detection limit of the method will be considered as a single rock. A different set of model-blocks has been

elaborated with the same methodology used in the elaboration of the blocks representing gypsum rocks of the section 4.1.4. In this new set of models, instead of a regular distribution of squares, an irregular distribution of little rectangles has been used (figure 5.11). The electrical resistivity of the bulk rock has been calculated following the same method, this is, performing the direct model and inverting afterwards with 18 iterations.

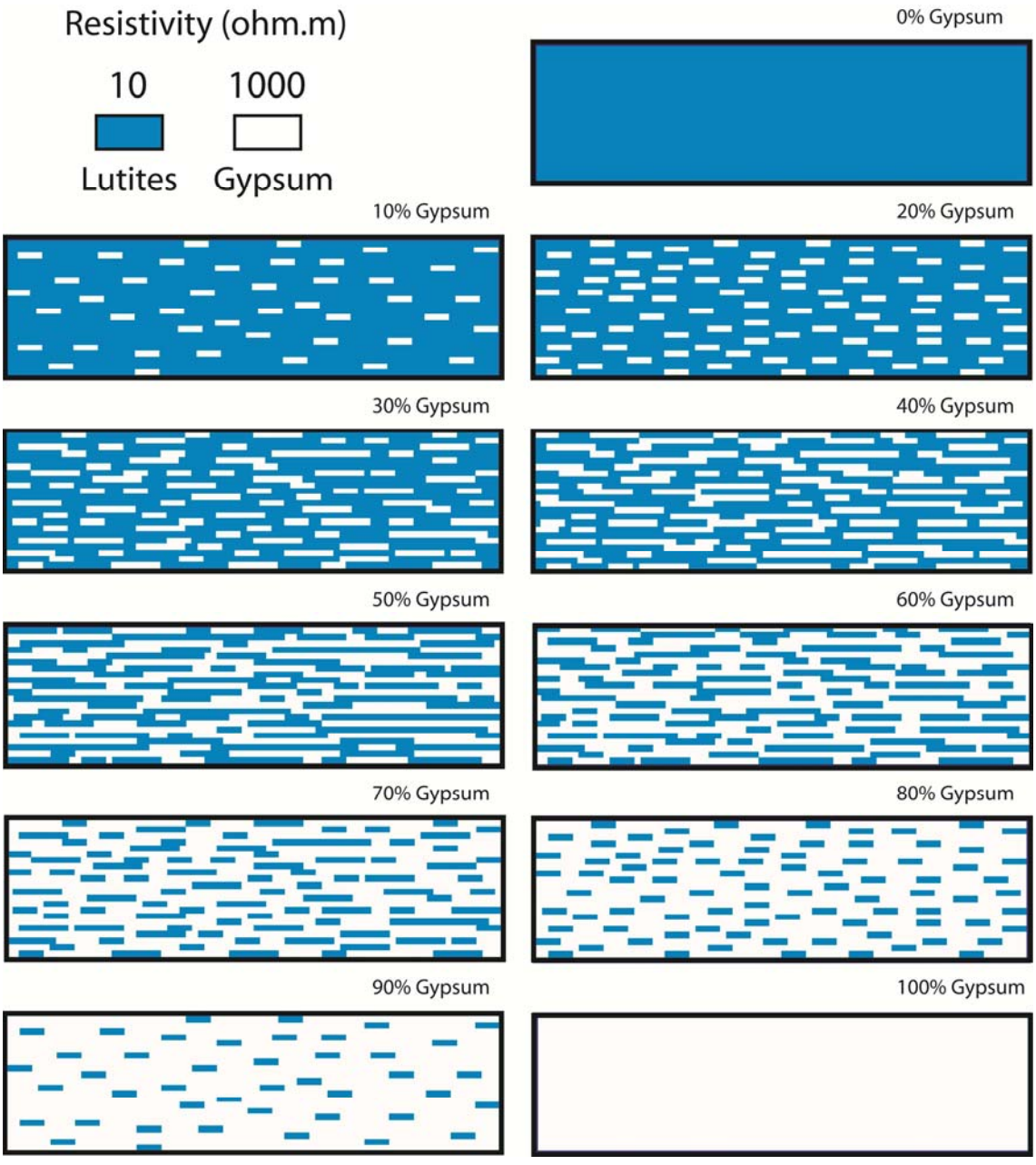

Figure 5.11: Model blocks elaborated with the RES2DMOD program; each block represents a gypsum rock body with changing composition. The distribution of the phases is partially heterogeneous in comparison with the models of figure 4.10.

The result displays a similar trend to the one observed in the case of the homogeneously distributed squares, but the transition zone is wider in this second case (figure 5.12); with smoother slope of the line in this transition. The values in the case of the purest (75% or above in purity) and impurest (30% or below in purity) rocks are similar. Thus, the heterogeneities in the distribution of the phases only affect to the transitional domain. The more heterogeneous is the distribution, the wider is this domain; but in no case will have a range wider than 25 to 75% in purity. This is due to the fact that when the presence of one phase is 75% or more, this phase will be the dominant one at any distribution. The effect of the heterogeneities in the electrical resistivity is the same for any combination of sulphate phases with matrix.

Another possible case is a layered deposit in which every layer has different purity in the sulphate phase. If the difference among purities is low, which is the most common case, the whole sequence can be considered as a single member with a mean purity. Examples of this are the previously mentioned gypsum formations of Vilobí and Cervera (profiles B and D respectively in figure 4.2 and 4.3). Rarely sulphate deposits have great variations of purity from layer to layer forming a heterogeneous sequence. Sudden variations in the purity exist; but normally are associated to the limit of a sequence or a stable change in the deposition conditions. In the case of having layering between almost pure matrix and highly pure sulphates, the transition zone will increase as in the case of heterogeneous distribution. This will be further discussed for chloride rocks in the next section.

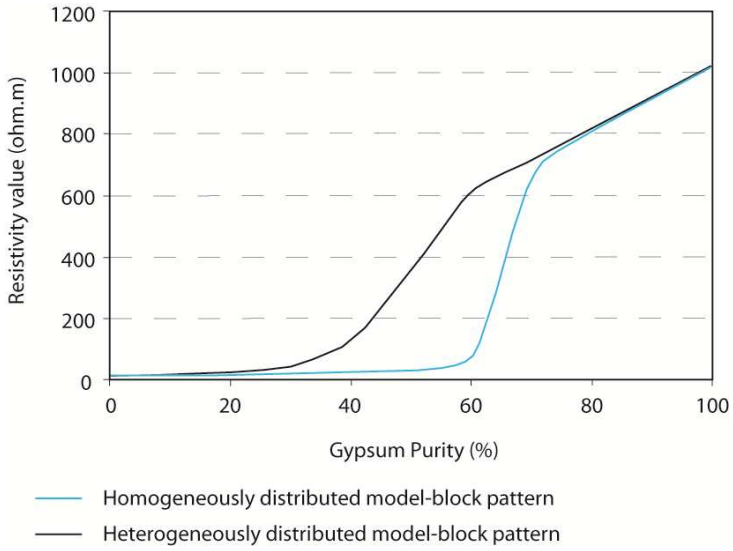

Figure 5:12: Electrical resistivity trends calculated theoretically for both homogeneously and heterogeneously distributed phases. The values have been obtained inverting the direct model with 18 iterations.

.3.3 Other parameters affecting the conductivity of sulphate rocks

Besides the composition and the distribution of the components, there are other parameters as temperature (Mizutani and Kanamori 1967), pressure (Parkhomenko 1982) or humidity (Bekhit et al. 2008) that may affect to the conductivity of rocks and therefore to their resistivity value. In any case, these parameters have little influence in the case of sulphate rocks; although they have significance in laboratory essays as it has been shown. In the other hand, the parameter of heterogeneity is difficult to control. Because of this, the classifications and models performed in previous sections has to be considered as a reference for surveys in sulphate rocks, but the obtained results may differ slightly from what it is expected.

.4 SURVEYS IN CHLORIDES

.4.1 Introduction: electrical properties of chloride rocks

After sulphates, chlorides are the most abundant evaporitical minerals. The most common chlorides are halite (NaCl), sylvite (KCl) and carnallite ($KMgCl_3 \cdot 6H_2O$). Their deposition takes place from highly concentrated brines in shallow or deep evaporitical basins. Unlike sulphate rocks, chlorides tend to be deposited in very pure layers interbedded with pure lutitic layers (figure 5.13A); so its heterogeneity rate is large (Landrø et al. 2011). Comparing with sulphates, they are much more soluble; and because of that, is hard to find outcropping chloride deposits. Due to the high ductility and capacity to flow of chloride deposits, is common to observe complex folds and faults which can be easily observed thanks to the marked layering (figure 5.13B).

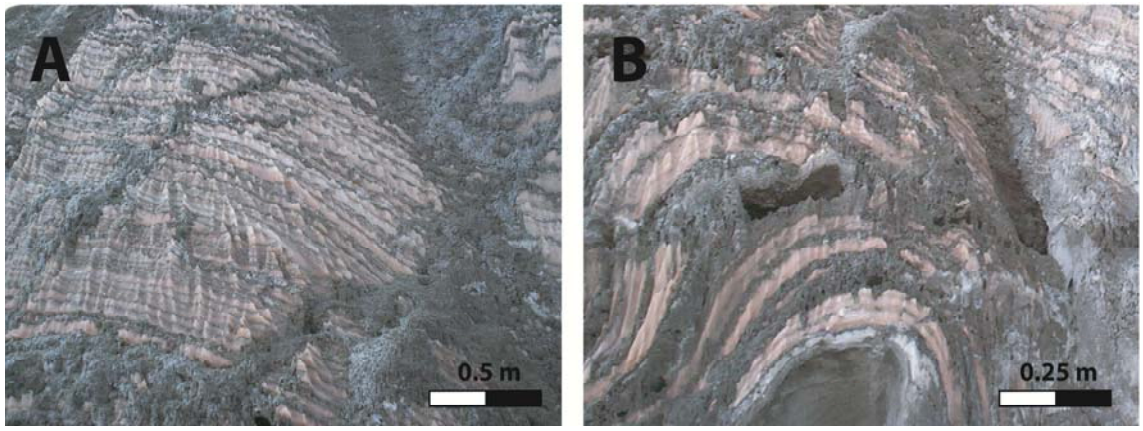

Figure 5.13: Photographs of chloride deposits in Cardona area: A) pure halite-pure lutite layering with some fractures filled with lutites; B) folds and faults of the chloride sequence.

From the geoelectrical point of view, the main difference between sulphate and chloride rocks is the lutite distribution within them. While in the case of sulphate rocks we have considered that as general trend they are homogeneous at metric scale (which fit to the most cases), in the case of chloride rocks we cannot assume that, if there is a high quantity of lutitic phase. This difference is based in the high contrast of layer composition, which affect greatly to the electrical percolation of these rocks. As it has been previously pointed, the sulphate rocks are usually deposited in different layers with different composition; but the compositional differences between layers are little (unless sulphate layers interbedded with

pure carbonates, which also occurs) and therefore the bulk electrical behavior of the deposit does not change. The interconnection of lutite phase in the chloride deposits is wider and more complex because it is not scattered in the chloride phase but concentrated in layers. Besides, due to the complexity of the deposits (fractures, faults and folds) the lutites tend to cross the pure chloride layers connecting the lutite ones.

As in the case of sulphates, the electrical resistivity of chlorides is not well defined. In any case, due to the heterogeneity of the deposits, the behavior is different comparing to sulphates. The percentage of each component will also change the conductivity of the bulk rock, but unlike the sulphates, the resistivity will not fit to the Hashin-Shtrikman bounds. Instead, transitional values between both bound are expected to be obtained as it has been shown in the previous section. Additionally to the compositional factor, the chloride rocks can contain abundant fluid inclusions (inter and intracrystalline). The presence of these brines affect greatly the electrical properties of the deposit due to their high conductivity, making a big difference between *dry* and *wet* chlorides.

.4.2 Field examples: geological settings and methods

The South Pyrenean fold-and-thrust belt is formed of various structures with different orientations detached above evaporitic levels (figure 5.14). These evaporitic levels were deposited during the Upper Eocene when the area was a foreland basin. The maximum thickness of the evaporitical deposits in the Cardona area was 300 meters in the center of the basin (Sans et al. 2003). Later, the evaporitic deposits were covered by continental Oligocene deposits during the compression period in which the deformation took place. Evaporitic materials shifted towards the cores of the anticlines forming diapiric structures. Nowadays a salt diapir outcrops in the area of Cardona forming a *salt-mountain*. In Súria the salt does not outcrop but it is situated at shallow depth (few meters, depending on the area).

Three ERT profiles have been performed in the chloride formations of Cardona and Súria (two and one respectively). In Cardona, the studied areas have been the summit of the *salt-mountain*, situated in the south part of the village, and a topographically depressed area in which the salt outcrops (at the east of the village). In Súria, the performed ERT profile is situated in the riverbed of Cardoner River (which runs through both Súria and Cardona). A Syscal Pro switch with 48 electrodes has been used with a 5 and 10 meters spacing for Cardona

and Súria areas respectively. The selected electrode array is Wenner-Schlumberger in both cases.

Additionally to the electric imaging, three seismic tomography sections have been carried out in Súria in order to support the geoelectrical survey. A DAQ Link–III seismograph with 24 geophones with a spacing of 3 meters between them has been used. In total 9 shot-points were acquired with 9 meter separation between them. The inversion of the data set has been performed with the commercial software RAYFRACT. The sections obtained from the seismic tomography have been compared with the data of the ERT and the previous geological knowledge of the area.

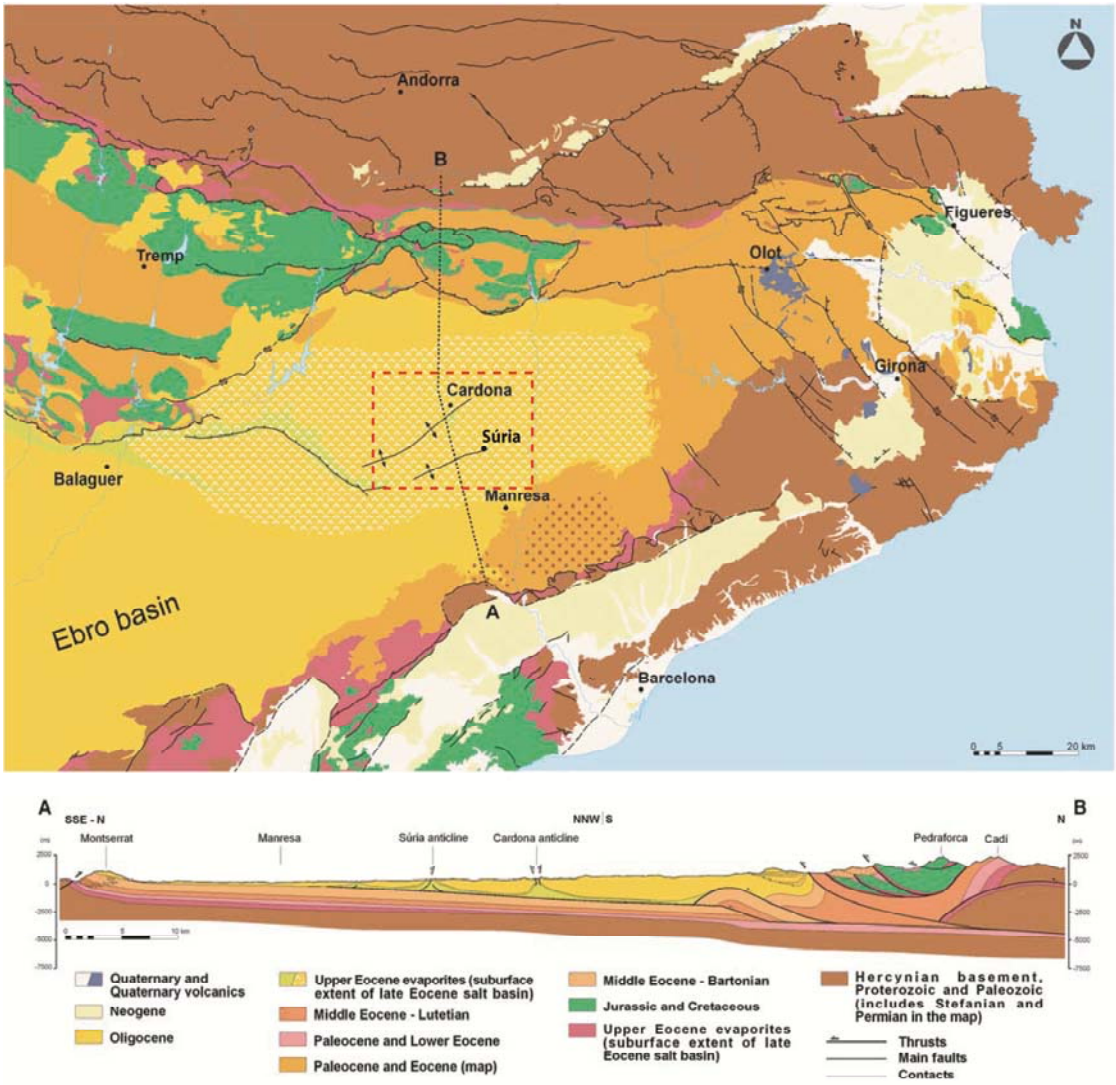

Figure 5.14: General geological map of the NE of Spain; the area of Cardona and Súria anticlines is marked with a red dashed line. In the section A-B (below), the structures of the Pyrenean thrust-system can be observed (modified from Landrø et al. 2011).

.4.3 Field examples: results and discussion

The first ERT profile was performed in the upper part of the *salt-mountain* of Cardona, where the salt is below an unconsolidated sediments layer (figure 5.15A). The inverted resistivity image (figure 5.16A) shows three different layers. The uppermost layer corresponds with the caprock; it shows resistivity values between 50 and 100 ohm.m. Below, the resistivity decreases to less than 5 ohm.m. In the lower part of this low-resistive material, two arched features are shown in which the resistivity increases progressively with depth. This layer corresponds with the salt formation. The caprock is permeable; thus, water runs through it and goes within the salt rock. This water may dissolve part of the salt, but once it is saturated, it remains as salty water. This water is the cause of the low resistivity showed in the upper part of the salt deposit. In depth, the salt is progressively drier, increasing the electrical resistivity. In any case, the dry salt displays electrical resistivity values lowers than it should be expected (<100 ohm.m); this is due to the previously mentioned impurities, which can be observed in the base of the *salt mountain*. This dry salt probably bears certain quantity of brine within because the amount of lutites in the salt formation has been observed in a mine below the *salt-mountain* showing lutite levels of averagely 1 mm comparing with the halite levels of averagely 5 mm. This quantity of lutites (less than 20% of the bulk composition of the deposit) does not explain itself the observed resistivity (too low for the expectable one), even considering the percolation of this material. On the other hand, the studied materials are at shallow depth (up to 50 m in Cardona area) and they may be affected at some term by dissolution and infilling of the materials which are above, making the purity in halite of the rock decrease locally.

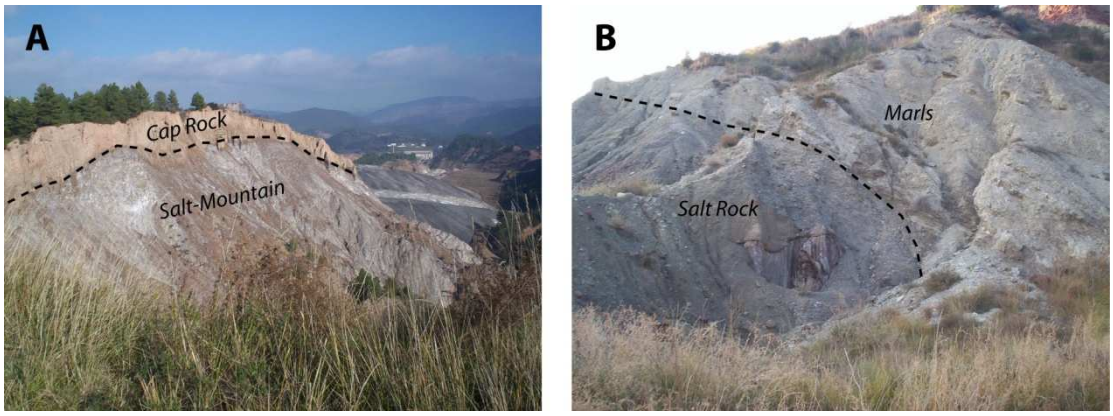

Figure 5.15: A) General view of the salt-mountain of Cardona in which the ERT profile A (figure 5.16A) has been performed. B) Center part of profile B (figure 5.16B) where the salt rocks change laterally to marls.

The second profile in Cardona was carried out towards the east, close to the Cardoner River. The section was spread near an outcrop of salt (figure 5.13). From west to east, the salt disappears in the outcrop and the profile center was placed in this transition (figure 5.15B). The inverted resistivity image (figure 5.16B) shows an upper low resistivity terrain, corresponding to the clayly materials covering the salt where the survey took place. Below, in the left side higher resistive materials are shown (up to 150 ohm.m). To the right side, this layer shows a decreasing in the resistivity. This change represent the transition from dry salt (in the left) to marls (in the right). In the lowermost part of the profile, the resistivity decreases achieving less than 3 ohm.m. This level represents the phreatic level in which the terrain is saturated in water. As this water has a lot of dissolved salts, it is very conductive. The materials below of the dry salt deposit correspond with wet salt rock.

The resistivity image from the ERT performed in Súria (figure 5.16C), shows similar characteristics to the ones of Cardona. The uppermost layer corresponds to the alluvial materials of the Cardoner River Basin (40-70 ohm.m). Below, the salt appears with low

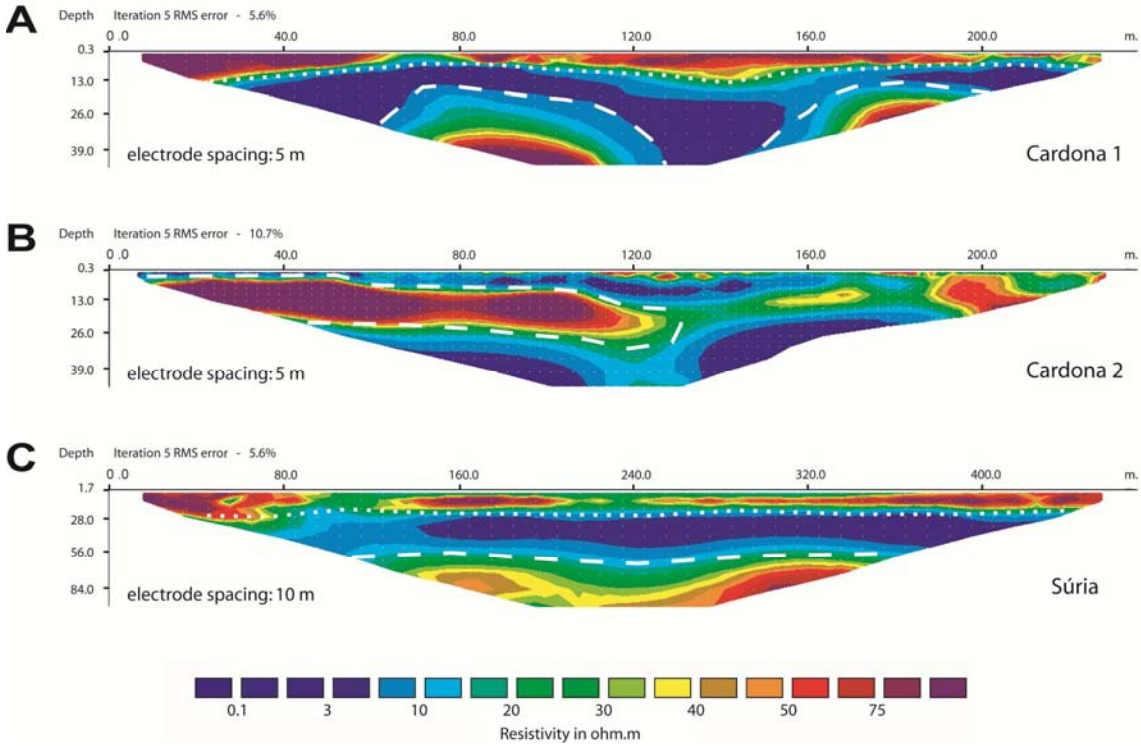

Figure 5.16: Inverted resistivity sections of the ERT profiles performed in Cardona (A and B) and Súria (C) areas. The dotted lines mark the boundary between wet salt rocks and covering materials; while the dashed lines indicate the areas with dry salt rocks.

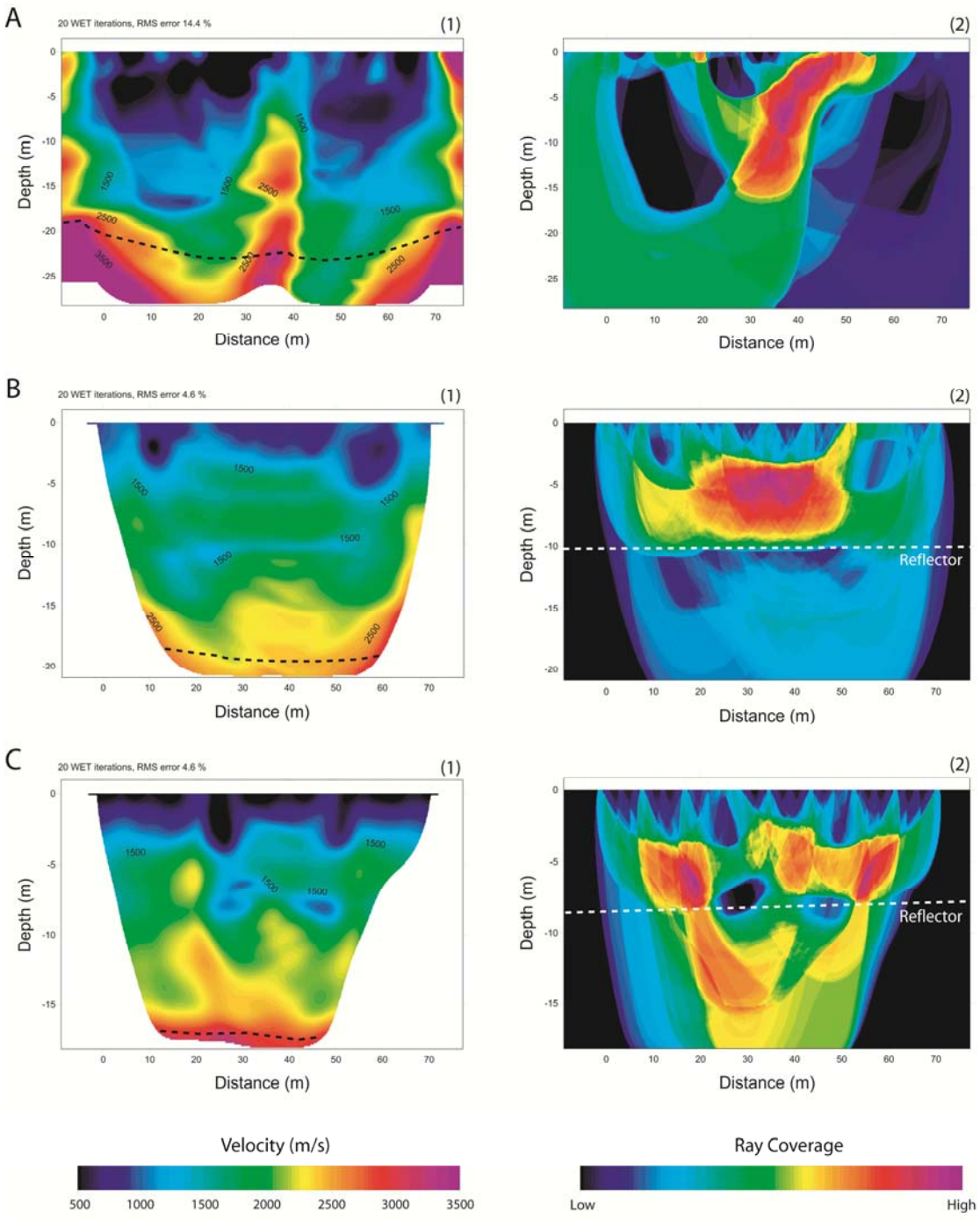

Figure 5.17: Seismic tomography sections (1) and their ray coverage (2) of Súria. Profiles A and B were performed in the same position as the ERT profile of Súria (figure 5.15C), while the profile C was performed close to them in a perpendicular position. The top of the salt rock is marked with a black dashed lines in the seismic tomography sections and the observed reflector is marked with a white dashed line in the ray coverage sections.

electrical resistivity values (<5 ohm.m) were the terrain is saturated in salty water, but higher values are displayed where the salt is relatively dry (at depth). In this area there is not

information from outcrops, but a borehole was performed in a previous survey and the salt was found at approximately 20 meters depth (Ribera F. pers. comm. 2010). Once again, the heterogeneity of the salt rocks makes the resistivity lower than the expected one.

In all the three studied areas the resistivity of the dry salt is close to 100 ohm.m, while in the case of salt is expected to be higher than 1000 ohm.m (Yamaranci and Flach 1992). This low values should be bounded to either (or a combination of both) certain contain in brine and a strong presence of lutitic levels.

The ERT profile of Súria has been supported with three seismic tomographic lines (figure 5.17). Two of them have been performed in the same position of the ERT profile; one to the left starting from the center of the profile (figure 5.17A) and the other to the right (figure5.17B). The third one is situated in the surroundings with perpendicular disposition respecting the other two (figure 5.17C). In any case, the geology of the area is simple with horizontal layers, so all three profiles show similar results. The data of the profile has an high RMS error (14.4%), but the area in which the coverage is medium-good can be observed that at depth, where the salt has been identified (at more or less 20 meters depth), the velocity increases up to more than 3500 m/s. The velocity for pure halite is 4500 m/s for the P-wave (Landrø et al. 2011). In profiles B and C the data is better and the RMS error is low (4.6% in both cases). Similar trend is observed with increasing in the velocity at 20 meters (which is the bottom of both profiles). In the ray coverage images a reflector is shown at 10 meter depth; this correspond to the transition in the Cardoner River basin from sand and gravels to marls which has been also observed in the borehole (Ribera F pers. comm. 2010). Hence; thanks to the seismic tomography is possible to distinguish the salt rocks from other materials due to their high velocity for P waves, but the presence of water cannot be estimated. Combining both ERT and seismic tomography is possible to obtain information of both parameters.